International Journal of High-Rise Buildings
December 2013, Vol 2, No 4, 345-354

International Journal of
High-Rise Buildings
www.ctbuh-korea.org/ijhrb/index.php

Advanced Structural Silicone Glazing

Jon Kimberlain[1†], Larry Carbary[1], Charles D. Clift[2], and Peter Hutley[2]

[1]*Dow Corning Corporation, 760 Hodgenville Road, Elizabethtown, Kentucky, 42701, USA*
[2]*Curtain Wall Design and Consulting, Inc., 8070 Park Lane Suite 400, Dallas, Texas, 75231, USA*

Abstract

This paper presents an advanced engineering technique using finite element analysis to improve structural silicone glazing (SSG) design in high-performance curtain wall systems for building facade. High wind pressures often result in bulky SSG aluminum extrusion profile dimensions. Architectural desire for aesthetically slender curtain wall sight-lines and reduction in aluminum usage led to optimization of structural silicone bite geometry for improved stress distribution through use of finite element analysis of the hyperelastic silicone models. This advanced design technique compared to traditional SSG design highlights differences in stress distribution contours in the silicone sealant. Simplified structural engineering per the traditional SSG design method lacks accurate forecasting of material and stress optimization, as shown in the advanced analysis and design. Full scale physical specimens were tested to verify design capacity in addition to correlate physical test results with the theoretical simulation to provide confidence of the model. This design technique will introduce significant engineering advancement to the curtain wall industry and building facade.

Keywords: Structural silicone glazing, Finite element analysis, Hyperelastic model, Building façade, Curtain wall

1. Introduction

Requirements for curtain walls have been influence by recent extreme wind events. Design wind speeds and cladding pressures have increased significantly resulting in correspondingly larger material sizes and material strength for sufficient structural capacity. For example, tall buildings in typhone zones have cladding pressures that now routinely exceed 6 kPa.

Over the last several decades, structural silicone glazing has successfully attached architectural glass to curtain wall framing in high performance building facades. Due to the increase in high pressures, the result has been an increase in bulky metal extrusion frame dimensions. Architectural desire to enable aesthetically slender curtain frame profiles and increased sight-lines prompted structural silicone designers to optimize the silicone sealant joint design.

The paper presents empirical and theoretical analysis of structural silicone design to develop a technique to design structural silicone glazed curtainwall for building façade.

2. Structural Silicone Glazing Yesterday and Today

Silicone structural glazing originated in 1965 with the use of glass-to-glass structural seals in the PPG Total Vision System. The practice further developed into two-sided applications in 1970, which utilized two sides of the glass infill adhered to metal framing members using silicone sealants, typically vertical jambs, with the head and sill of the glazing captured into a glazing channel with compression glazing. Four-sided applications, where silicone sealants were solely utilized to attach glass to metal mullions, were first utilized in 1971. Use of innovative glass products yielded two-sided and four-sided applications of insulating glass units in 1976 and 1978 respectively (Hilliard et al., 1977).

Structural silicone glazing has been studied with respect to high-performance environments for the last several decades with proven durability and performance in areas of high wind zones, hurricane/typhoon prone areas, extreme temperatures, and seismic activity (Carbary 2007).

However, the basic design theory on how to properly size the structural joint has remained the same. The bite calculation as derived from the trapezoidal loading theory is as follows

$$\text{Bite} = \frac{0.5 \times \text{short span length} \times \text{wind load}}{\text{Sealant design strength}}$$

The ASTM article, "Methods for Calculating Structural Silicone Sealant Joint Dimensions," published in 1989, discussed the structural joint width for a rectangular glazing unit is based on the simple physical relationship of the size of the glass, trapezoidal loading principle, maximum windload, and a maximum sealant design strength of 20 psi (Haugsby et al., 1989).

- The windload is the maximum determined force of

†Corresponding author: Jon Kimberlain
Tel: +011-1-270-706-8301; Fax: +011-1-270-706-8351
E-mail: jon.kimberlain@dowcorning.com

pressure due to wind speed
- Short span is the shortest dimension of the four sides of rectangular glazing unit
- Sealant design strength is the maximum tensile force allowed on the sealant

Sealant technology, analytical techniques, and computing technology has significantly advanced over the history of the practice of structural glazing. Sealant technology has progressed with neutral curing formulations, increased tensile strengths, and higher movement capability. Studies have been conducted on the performance of sealants in specialized applications. Several papers have been written on the use of silicone sealants in curtain wall units for seismic activity (Zarghamee et al., 1996) including the use of finite element analysis to predict the mode of failure in silicone joint (Broker et al., 2012).

A study entitled "Evaluation of Silicone Sealants at High Movement Rates Relevant to Bomb Mitigating Window and Curtainwall Design", used high-speed photography and specialized measuring devices that illustrated the relationship of the tensile capability of the sealant increases as the speed increases to validate the successful use in ballistic applications (Yarosh et al., 2008).

The basis for design strength and method of design are not addressed in these papers. For good reason, as the design has been used in projects over the world that has performed well in excess of 40 years. ASTM C1401 Standard Guide for Structural Sealant Glazing is the most complete reference to the design considerations for structural silicone glazing. This document provides an excellent overview of the practice along with a full list of historical references regarding the subject.

There have been efforts to challenge both the basis of designing structural joints and increasing design strengths as mentioned above. Unfortunately, there have been no thoroughly developed and published technical arguments for proof of challenges. Opportunistic approaches appear to be based on short-term business risks and rewards with no regard to impacts of durability based on sound science and engineering.

Finite element analysis of structural silicone has been used to explore standard (Travis et al., 1998) and unique designs (Hagl, 2008) coupled with the understanding of the non-linear behavior of structural silicone materials. This tool, which has been used in the aerospace and automotive industries, has expanded the understanding of non-linear materials in the construction industry.

3. Finite Element Modeling of SSG

Advanced computer software analysis can provide access to several hyperelastic material properties, as well as curve-fitting subroutines that can be used to automatically generate material property data from physical testing. The services of Axel Products were used to develop accurate tension, shear, and biaxial extension data for Dow Corning (R) 983 Structural Glazing Sealant material. The Axel data models for tension, shear, and biaxial data were then curve-fitted with several material models within the software analysis to find a curve fit which minimized the scaled residuals resulting from the data provided. An incompressible two-parameter Mooney-Rivlin curve fit was selected because it produced minimal scaled residuals. Independent literature indicates that the Mooney-Rivlin material model can accurately represent a material's response up to 100% strain.

The Mooney-Rivlin two parameter model was tested against the results of ASTM C1135 tensile adhesion joint samples by Dow Corning to validate the generate model using a 1.27 mm mesh size. Below documents the model used to replicate the ASTM C1135 test sample where the size of the silicone joint was 50.8 mm × 12.7 mm × 12.7 mm. For computational efficiency, the size of the glass adhered to the silicone was reduced to the surface area of the silicone sample itself.

Results of the ASTM C1135 test model were compared to the results of physical specimens of the same batch of

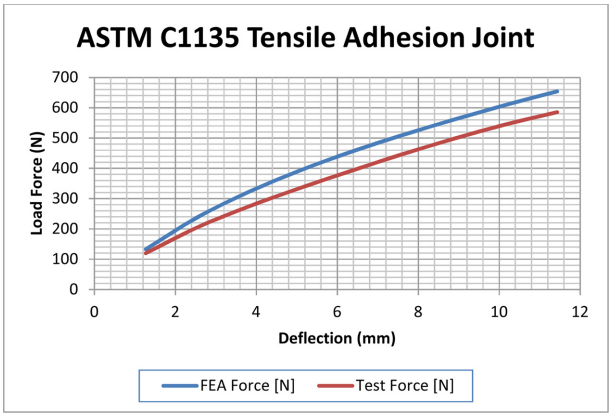


Chart 1. Induced load versus sample deflection in ASTM C1135 Tension Tests (typical of 12.7 mm × 12.7 mm × 50.8 mm joint size).

Table 1. Estimated error between load determined in the FEA Model and actual load test from specimen prepared with silicone batch used in FEA data model

Error Within Silicone Batch			
Deflection [mm]	FEA Force [N]	Test Force [N]	Percent Error
1.27	133	120	11.2
2.54	238	205	15.7
3.81	322	274	17.6
5.08	393	335	17.4
6.35	455	392	16
7.62	510	447	14.3
8.89	561	498	12.8
10.16	609	545	11.7
11.43	654	585	11.9

Table 2. Estimated error between loads determined in ASTM C1135 modeled in FEA and actual results of three historical batches of ASTM C1135 testing

Error Between FEA and Silicone Batches							
Strain (%)	Force [N]				Percent Error		
	FEA	Batch 1	Batch 2	Batch 3	Batch 1	Batch 2	Batch 3
25	133	173	200	162	-22.9	-33.3	-17.6
50	290	352	347	282	-17.7	-16.4	2.7
75	455	573	533	429	-20.6	-14.6	6.1

silicone used in the Axel Products curve-fitted data. Chart 1 documents the load vs. deflection diagrams of the ASTM C1135 test results and the C1135 ANSYS FEA results. Additionally, results at each 1.27 mm of deflection are provided in Table 1, along with the resultant force error at each point.

The results within the curve-fitting regime in a single silicone batch indicated a maximum recorded error of 17.6% in the range of 3.81 mm deflection, or approximately 30% nominal strain. In all cases, the FEA results over-predicted the physical test results. Observation of the percent error within the silicone batch indicated that while the material properties appeared stiffer than the material tested, the offset between the tested and modeled materials is consistently between 11% and 18% through the modeled extensions. It should be noted that the strain rate of the data used to generate the FEA material properties and the data used to generate the ASTM C1135 test results were different; the FEA material properties were generated at 0.01 s^{-1} strain rate, while the ASTM C1135 test results were generated at 0.0167 s^{-1} strain rate. It is known that rate of strain of hyperelastic materials affects the modulus properties; the effects of the rate of strain were not explicitly analyzed in this paper [Yarosh et al.].

FEA results were compared across several batches of silicone in addition to the single batch above (Table 2). Dow Corning provided three randomly selected data sets from individual batches for error analysis. Results of the sensitivity study indicate the error between the FEA silicone model and the sample batches has a maximum reported error of 33.3% at 25% strain. Unlike the intra-batch comparison, the inter-batch comparison indicates the FEA model is under predicting the induced loads in the physical tests. The error calculated from the inter-batch comparison lacks the consistent offset between the two materials of the intra-batch study. Again, it should be noted that the strain rate of the historical data was generated at a different load rate than the strain rate of the FEA model. The historical data was generated at a load rate of 50.8 mm/min, equal to a strain rate of 0.067 s^{-1}.

Stress distribution plots in Figs. 1 and 2 indicate the results of the FEA models at 0.76 mm deflection and 1.78 mm deflection. At these deflections, the induced forces were 84.1 N and 177.9 N, respectively, which are approximately representative of 100% and 200% of what is typically considered limiting stresses for structural silicones.

Note that in both cases, stress peaks are calculated around the perimeter, and the stress within the silicone sample is highly non-uniform. The high differential stiffness between the silicone and the adjacent substrate causes the stress to be unevenly distributed. The results shown above are consistent with typical failure propagation start-

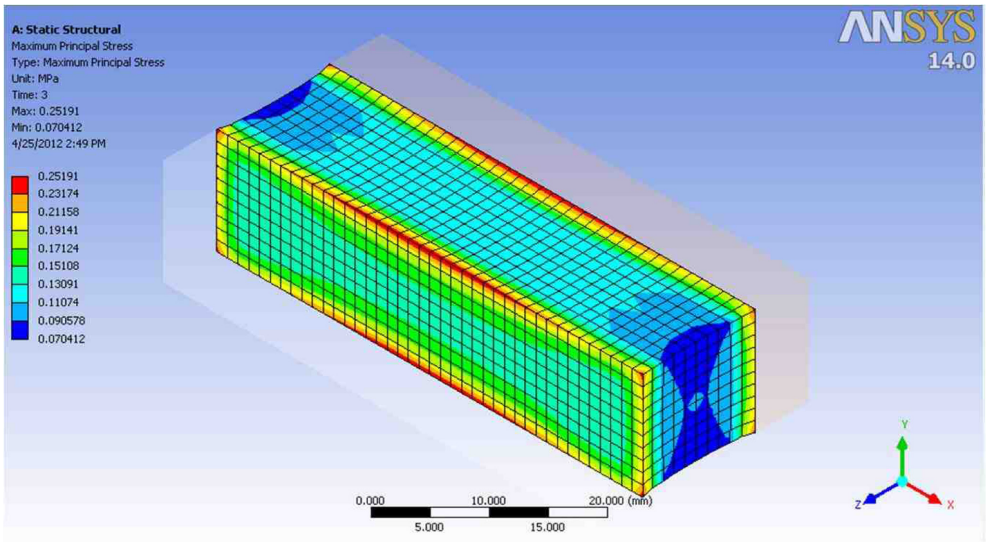


Figure 1. Distribution of Stress at 100% of Allowable Nominal Silicone Stress.

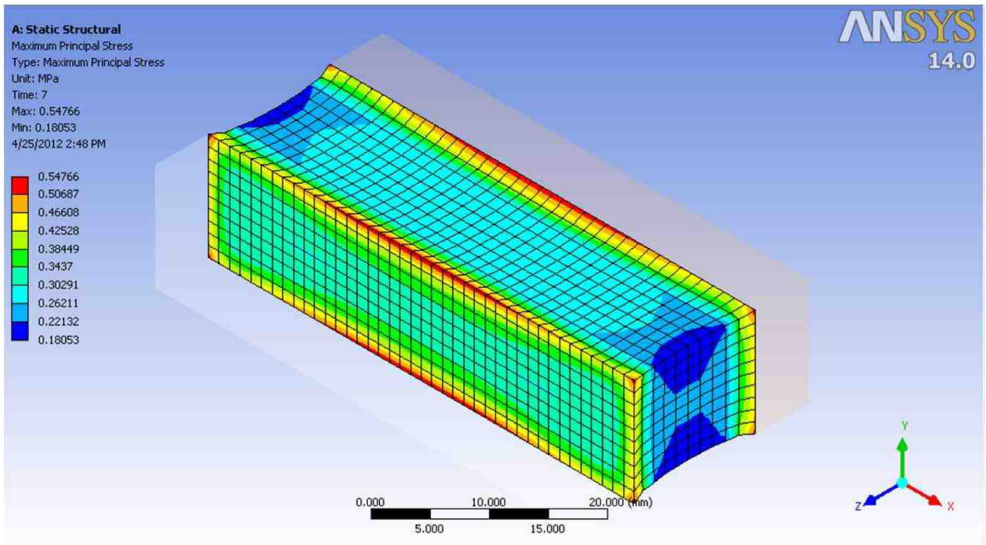


Figure 2. Distribution of Stress at 200% of Allowable Nominal Silicone Stress.

ing at the perimeter of the testing specimen as observed in ASTM C1135 tests.

The rationale behind the newly proposed silicone sealant joint can be seen in the results of the ASTM C1135 test samples. In a typical curtain wall assembly under negative loads, where the silicone is adhered in a square geometry, the finite rotation of the glass at the perimeter seal will induce the greatest movement at the edge of the silicone joint. The concept behind the new sealant geometry design allows additional movement capacity for the glass to rotate more freely rather than forcing the sealant to fight against the finite rotation of the glass at the perimeter (theoretically inducing a moment couple within the sealant). Fig. 3 schematically demonstrates the anticipated center of rotation of the glass relative to the silicone joint in both cases.

The proposed sealant joint design was tested on a 1905 mm × 1524 mm glass model. One quarter of the glass was included in the model for computational efficiency. Two models were generated: one for the proposed sealant design (trapezoid with 23.81 mm long dimension, 6.35 short trapezoid dimension, and 12.7 mm long trapezoid dimension), and one with a 50.8 mm long rectangular sealant joint, per

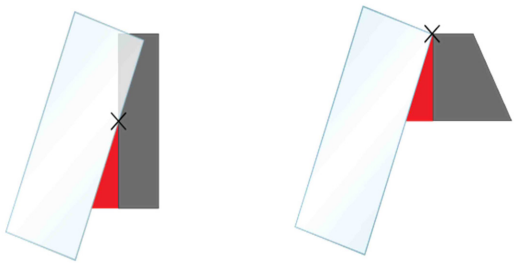


Figure 3. Assumed Glass Rotation for Trapezoidal and Traditional Silicone Joints.

standard industry practice. The glass was loaded to 9.6 kPa. The results of the models were compared as well as to benchmark stresses in the C1135 model.

The results of the trapezoidal silicone models that indicate maximum stress through the gross area of the silicone bite did not exceed 0.38 MPa, with peak stress along the edge of the silicone joint at 0.64 MPa. The results of a similar ASTM C1135 test sample with similar edge stresses were loaded to 2.29 mm deflection and 218.6 N applied force. The results of a "traditional" silicone model indicate the gross area of the silicone bite did not exceed 0.55 MPa, with peak stress along the edge of the silicone joint at 0.91 MPa. The results of a similar ASTM C1135 test sample with similar edge stresses were loaded to 3.30 mm deflection and 293.4 N applied force. Details of these stresses at the mid-span of both the long and short dimensions, as well as comparable peak edge stresses are shown in Figs. 4 to 9.

The results of the preceding figures indicate that a stress reduction can be achieved by allowing the silicone to rotate with the glass under large wind loads. It also shows that safety factors included in the design of silicone joints may not be as high as those indicated when comparing silicone in the traditional configuration to the results of a C1135 sample test.

To confirm that the proposed silicone joint would not compromise the glass under positive loads, the above-mentioned silicone joint was loaded to 6.2 kPa positive pressure to check the effects on the stress distribution within the silicone joint. Corner joint stresses were checked against the stresses in the typical silicone joint; these can be seen in Fig. 10. The stresses in both the gross area and the corner of the trapezoidal silicone joint did not exceed those in the traditional silicone joint under negative wind loads.

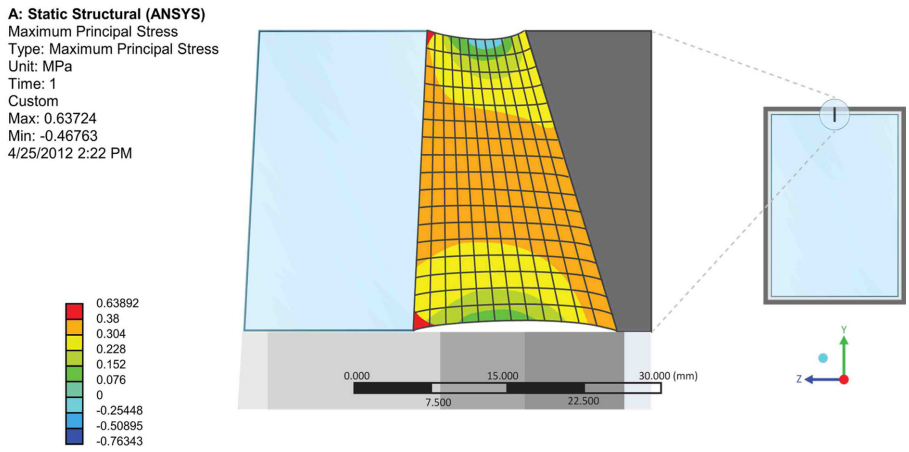


Figure 4. Distribution of Stress at Short Dimension Midspan of Trapezoidal Joint at 23.8 mm orthogonal bond width between glass and sealant.

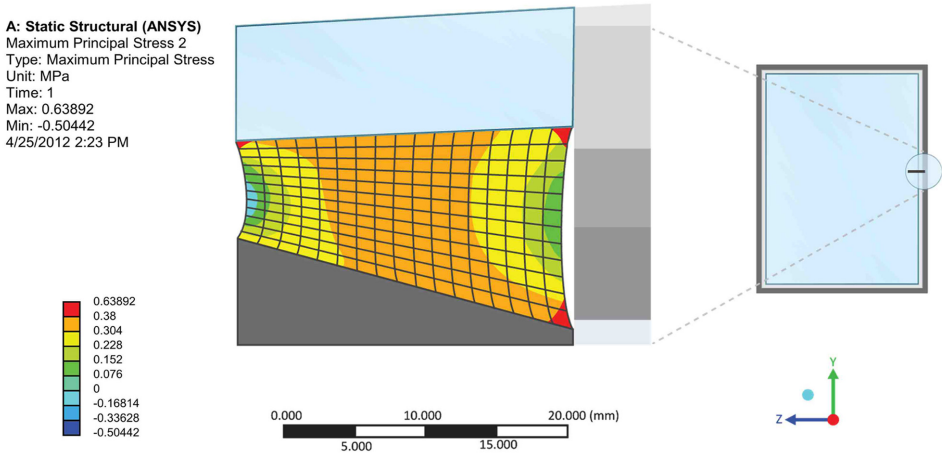


Figure 5. Distribution of Stress at Long Dimension Midspan of Trapezoidal Joint at 23.8 mm orthogonal bond width between glass and sealant.

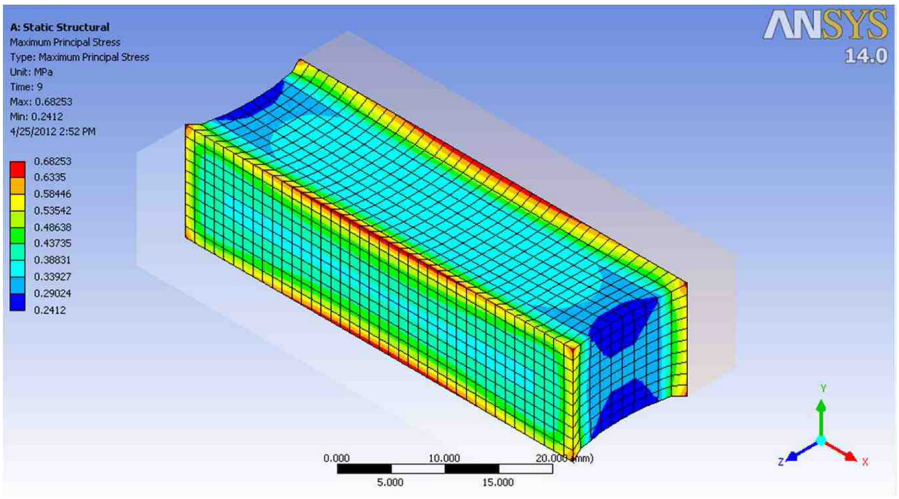


Figure 6. Test Results of ASTM C1135 Tensile Adhesion Joint (typ. 12.7 mm × 12.7 mm × 50.8 mm) with Similar Peak Edge Stresses to Trapezoidal Joint.

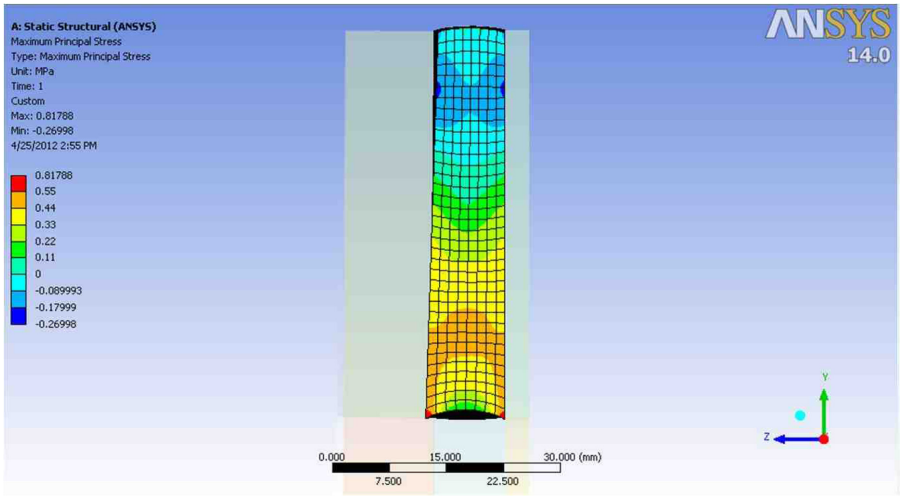


Figure 7. Distribution of Stress at Short Dimension Midspan of Traditional Joint at 50.8 mm bond width.

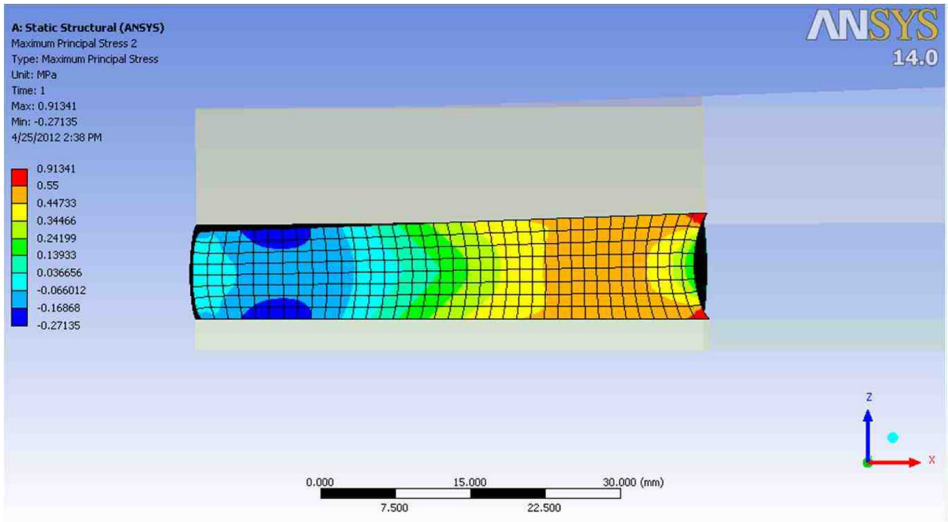


Figure 8. Distribution of Stress at Long Dimension Midspan of Traditional Joint at 50.8 mm bond width.

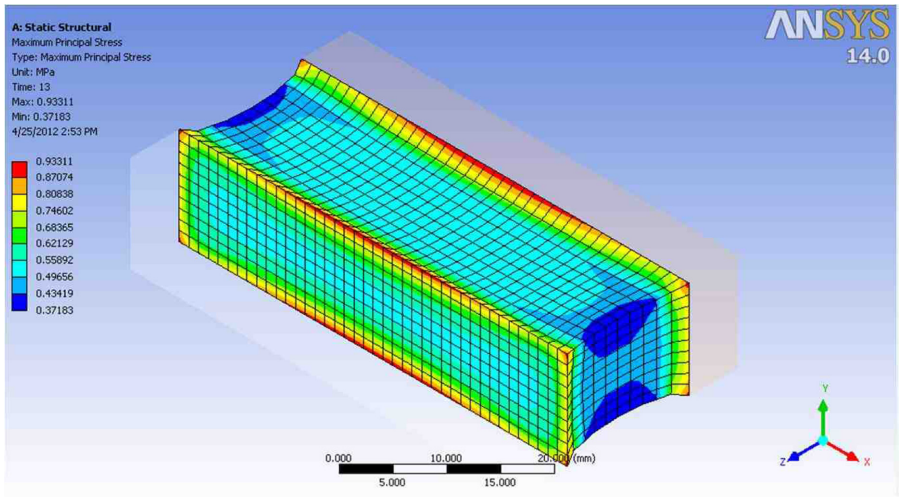


Figure 9. Test Results of ASTM C1135 Tensile Adhesion Joints (12.7 mm × 12.7 mm × 50.8 mm) with Similar Peak Edge Stresses to Traditional Joint.

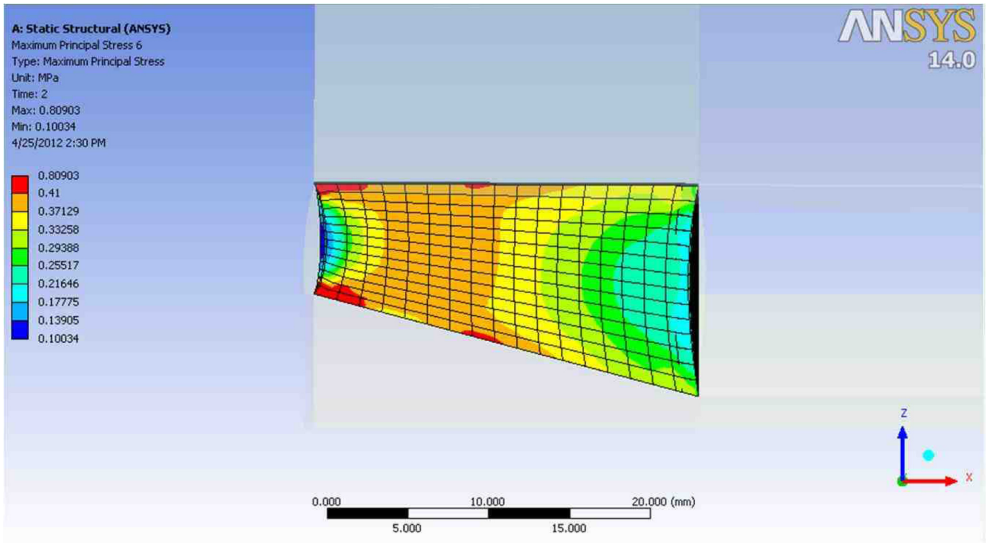


Figure 10. Distribution of Stress at the Corner of the Trapezoidal Silicone Joint under Positive Wind Load (23.8 mm orthogonal bond width).

4. Mock Up Results

The unique joint design was scaled up on a real size piece of glass and a design of 9.58 kPa (200 psf) and tested to the Miami Dade, Florida Building Code's Test Protocol for High-Velocity Hurricane Zones. The protocols that were followed were Testing Application Standard (TAS) TAS 202-94, the procedure for conducting uniform static air pressure test. This test is operated in the spirit of ASTM E330 Standard Test Method for Structural Performance of Exterior Windows, Doors, Skylights and Curtain Walls by Uniform Static Air Pressure Difference.

The loading pressures for this mockup were 9.58 kPa (200 psf) with a 14.37 (300 psf) test to validate 150% overload as specified in the TAS 202-94. The mockup samples were fabricated to accommodate a glass size of 1524 × 1905 mm (60 × 75). Two different laminates we used, Polyvinylbutyral (PVB) and DuPont SentryGlas Plus (SGP). Three different monolithic laminated types of glass were used in the mock up testing.

1. 5 mm clear tempered, 2.3 mm PVB interlayer, 5 mm clear tempered (3/16 Clear tempered, 0.090 PVB interlayer, 3/16 Clear tempered)
2. 5 mm clear tempered, 2.3 mm SGP interlayer, 5 mm clear tempered (3/16 Clear tempered, 0.090 SGP interlayer, 3/16 Clear tempered)
3. 6 mm clear Heat Strengthened, 2.3 mm SGP interlayer, 6 mm clear Heat Strengthened (¼" Clear Heat Strengthened, 0.090 SGP interlayer, ¼" Clear Heat Strengthened).

The glass was attached to an anodized aluminum frame as shown in Fig. 11 with a 23.8 mm structural bite orthogonally projected through the trapezoidal joint configuration. Conventional calculation would have required a minimum structural bond width of 52.9 mm. The frame was constructed out of a standard aluminum tube to which a

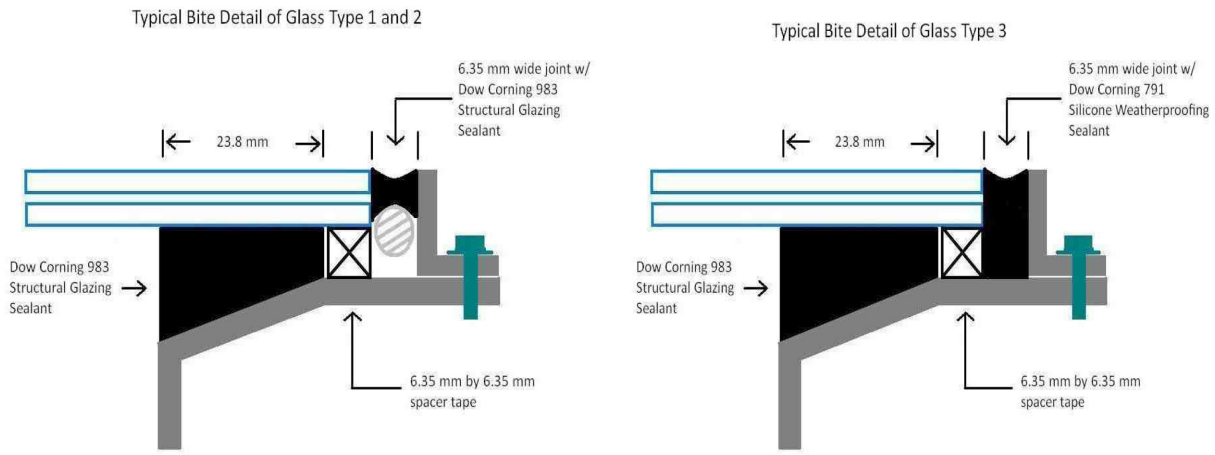


Figure 11. Detail of horizontal and vertical attachment in tested mockups.

Table 3. Deflection measurements of unitized curtain wall units under negative and positive windload during TAS 202 testing method. Glass type corresponds to glass and laminate configurations listed in above text. Glass Type 1 comprised of Tempered and PVB, Glass Type 2 comprised of Tempered and SGP, and Glass Type 3 comprised of Heat Strengthened and SGP

Deflections (mm)	Top Corner			Mid Point of Long Span			Bottom Corner			Center of Glass		
	Glass Type 1	Glass Type 2	Glass Type 3	Glass Type 1	Glass Type 2	Glass Type 3	Glass Type 1	Glass Type 2	Glass Type 3	Glass Type 1	Glass Type 2	Glass Type 3
50% of Test Pressure 7.19 kPa (+150 psf)	3	5.3	6.6	4.3	6.6	6.6	3.8	4.6	4.1	26.9	21.1	16.8
Permanent Set	2.3	3.3	1	2.3	3.3	1.3	2.3	2.8	1.5	4.1	3	1.3
Design Pressure 9.58 kPa (+200 psf)	3.6	6.1	7.1	5.6	8.1	8.1	4.8	5.6	5.6	31.8	25.7	21.1
Permanent Set	2.8	3.8	1	2.8	3.8	1.5	2.8	3	1.8	5.3	3.6	1.5
50% of Test Pressure -7.17 kPa (-150 psf)	5.1	2.5	2.8	6.1	4.8	5.8	5.3	4.6	6.4	34.5	22.6	19.6
Permanent Set	3.8	0.8	0.5	3.8	1.8	0.8	3.6	2.5	0.8	6.1	2.3	1.3
Design Pressure -9.58 kPa (-200 psf)	6.1	3.8	5.6	7.9	6.6	8.6	6.9	5.8	8.1	39.9	27.7	23.1
Permanent Set	4.3	1.5	1.5	4.1	2.3	1.5	3.8	2.8	1.5	6.1	3	1.5
Test Pressure 14.37 kPa (+300 psf)	9.4	8.1	9.1	12.4	11.2	11.4	10.9	7.9	8.1	44.5	33.3	29.2
Permanent Set	6.9	4.6	1.3	7.6	4.6	1.5	7.4	3.3	1.5	9.9	4.1	2
Test Pressure -14.37 kPa (-300 psf)	5.6	7.4	7.6	8.1	11.2	11.9	6.9	8.6	10.2	45.5	36.6	29.7
Permanent Set	1.3	2.3	1.5	1	3	2	0.8	3.6	1.3	4.6	3.8	1

Table 4. Performance data for mock-up assemblies for air infiltration, water infiltration and forced entry

Curtain Wall Assembly	Air Infiltration at 75.2 Pa (1.57 psf, 25 mph)	Air Infiltration at 300 Pa (6.24 psf, 50 mph)	Water Infiltration at 15% Positive Design Pressure (1.44 kPa, 30 psf)	Forced Entry - ASTM F588-07
Glass Type 1 - Tempered and PVB Laminate	<0.18m^3/m^2/hr (<0.01 cfm/ft^2)	<0.18m^3/m^2/hr (<0.01 cfm/ft^2)	No Penetration	Pass
Glass Type 2 - Tempered and SGP Laminate	<0.18m^3/m^2/hr (<0.01 cfm/ft^2)	<0.18m^3/m^2/hr (<0.01 cfm/ft^2)	No Penetration	Pass
Glass Type 3 - Heat Strengthened and SGP Laminate	<0.18m^3/m^2/hr (<0.01 cfm/ft^2)	<0.18m^3/m^2/hr (<0.01 cfm/ft^2)	No Penetration	Pass

brake metal shape was mechanically attached with 6 mm (¼") fasteners 200 mm (8) on center. Glass type 1 and 2 were tested exactly as shown in Fig. 1. The weatherseal detail used with glass type 3 was altered by omitting a backer rod and filling the rectangular cavity with the structural silicone. In all cases the structural silicone was not in contact with the silicone used at the glass edge.

During test deflection, measurements were taken of the aluminum frame and the center of glass at the testing laboratory. These deflections are reported in Tables 3 and correspond to the locations noted in the table specific to the glass type listed above.Tables 3 and 4 report the data taken on the air infiltration, water infiltration, and static loading of the glass units.

The three types of glass met the Miami Dade Code requirements for TAS 202-94 at a design wind pressure of 9.58 kPa (200 psf) which included a 14.37 kPa (300 psf) overload.

This mock up (shown in Fig. 12) clearly showed that the unique silicone joint design passed the windload design



Figure 12. Picture of actual mock-up assembly used in testing validation.

criteria for 9.58 kPa (200 psf) and survived the 14.37 (300 psf) overload. The silicone material used for the structural attachment of the glass in combination with the unique joint design has demonstrated the potential to perform beyond current accepted methods for SSG design.

5. Conclusions on Superior SSG and Incorporating a New Design

As mentioned previously, the lack of credible technical publications has created a need to properly consider new design methods or increases to design strength of structural silicone sealant. The following is a proposed method for a credible and systematic approach for use of Finite Element Analysis for advanced design of structural bite configuration and appropriate maximum stresses beyond traditional.

1. Establish an accurate FEA model
2. Develop an FEA model of a structural joint designed by the conventional formula and design stress
3. Develop an optimized FEA model for the alternative joint design and sealant design strength
4. Compare conventional joint models and alternative models to determine that distribution of maximum stress has been reduced via alternative design
5. Validate alternative joint design with actual performance mock-up curtain wall units

Finite Element Analysis models are generated by complex computing software that requires two main components. First and foremost is the proper selection of a material model that accurately predicts the behavior of a material over the range of expected performance. Second is an accurate data set that has been tested by conventional test methods recognized by the modeling software to accurately predict real world performance of the material.

Tensile adhesion joints tested to ASTM C1135 have become a standard test method to understand the stress/strain relationship of structural sealants in a prototypical SSG joint geometry in curtain wall units. Given the proven history of the conventional structural design methods with correlation to predicted material performance of a tensile adhesion joint, one should be convinced that the selection of the proper model for predicting material behavior would be predictive of the performance of the tensile adhesion joint.

Next in the process for alternative design would be to predict the distribution of forces in a conventional joint design at maximum loads. Understanding the peak forces generated in a tensile adhesion joint stressed to design load is very important.

Using the FEA modeling software, the next step would be to determine the optimal joint geometry to predict an overall lower cumulative stress distribution within the sealant joint to achieve desirable conditions for reduced aluminum or metal framing members without sacrifice to damaging loads to the structural silicone sealant's capability.

Comparison of both models should make physical sense with respect to the expected performance of the sealant including actual test results, reasonable expectation for forces generated within the different joints, and appropriate validation of the different joint geometries such as the tensile adhesion joints tested according to ASTM C1135.

ASTM C1184 outlines the needed performance of a silicone sealant used in structural glazing applications. Of importance is a minimum tensile property of 350 kPa (50 psi) as tested by ASTM 1135 at different potential environmental conditions related to temperature and environmental exposure. Silicone sealants are well behaved over a wide range of expected temperatures, but potential differences exist within the performance expectations of the sealant.

This illustrates an important consideration in selection of the sealant used for alternative joint design. Structural sealants that marginally meet any requirement of ASTM C1184 via ASTM C1135 testing should not be considered as a primary option relative to other choices. Sealants that meet each requirement with a relatively high safety factor should be the primary choices for alternative design and sealant design strength.

Mock-up testing should be used to enable predictive comparison of the actual sealant behavior and predicted behavior from the FEA model to ensure the competency of any deviation from the convention of our current standard that has proven 40+ years of success. Performance to onetime events such as bomb blasts and impact applications still will need proper consideration from current practices of testing actual mock-ups for appropriate building codes and industry accepted test methodologies.

References

Broker, K. A., Fisher, S. and Memari, A. M. (2012). "Seismic Racking Test Evaluation of Silicone Used in a Four-Sided Structural Sealant Glazed Curtain Wall System, *Journal of ASTM International*, 9(3), March 2012 Paper ID JAI104 144, Available online at www.astm.org

Carbary, L. D. (2007). A Review of the Durability and of Performance Silicone Structural Glazing Systems, Glass Performance Days 2007, Conference proceedings http://www.glassfiles.com/library/article.php?id=1083&search=carbary&page=1 (viewed April 23, 2012)

Hagl, A. "Durability by Design: New Results on Load Carrying Silicone Bonding. 2008: Third Symposium on Durability of Building and Construction Sealants and Adhesives, Denver CO, June 25-26, *Journal of ASTM International* 9(2), Paper ID JAI101956 Available online at www.astm.org

Haugsby, M. H., Schoenherr, W. J., Carbary L. D. and Schmidt, C. M. (1989). "Methods for Calculating Structural Silicone Joint Dimensions, Science and Technology of Gla-

zing Systems, ASTM STP1054, C. J. Parise, Ed., American Society for Testing and Materials, Philadelphia, pp. 46-57.

Hilliard, J. R., Parise, C. J. and Peterson, C. O. Jr. (1977). Structural Sealant Glazing*, Sealant Technology in Glazing Systems, ASTM STP 638,* ASTM International, West Conshohocken, PA, pp. 67-99.

Travis, H. S. and Carbary, L. D. (1998). "Finite Element Analysis of a Structural Silicone Shear Bead used in Skylight Applications, Science and Technology of Building Seals, Sealants, Glazing and Waterproofing: Seventh Volume, ASTM STP 1334, Jerome M. Klosowski, Ed., American Society of Testing and Materials,..,

Yarosh, K. F., Wolf, A. T. and Sitte, S., "Evaluation of Silicone Sealants at High Movement Rates Relevant to Bomb Mitigating Window and Curtainwall Design 2008, *Journal of ASTM International*, Vol. 6, No. 2, Paper ID JAI101953, Available online at www.astm.org

Zarghamee, M. S., Schwartz, T. A. and Gladstone, M. (1996). "Seismic Behavior of Structural Silicone Glazing," *Science and Technology of Building Seals, Sealants, Glazing, and Waterproofing, Sixth Volume, ASTM STP 1286*, ASTM, pp. 46-59.